

INTERIM REPORT IR-98-069/September

Wheat Yield Functions for Analysis of Land-Use Change in China

Cynthia Rosenzweig (cccer@cheops.giss.nasa.gov)

Ana Iglesias (iglesias@ppr.etsia.upm.es)

Günther Fischer (fisher@iiasa.ac.at)

Yanhua Liu (liuyh@acca21.edu.cn)

Walter Baethgen (baethgen+AEA-undp.org.uy)

James W. Jones (jwj@agen.ufl.edu).

Approved by

Gordon J. MacDonald (macdon@iiasa.ac.at)

Director, IIASA

Contents

Abstract	iii
Acknowledgements	iv
About the Authors	v
Introduction	1
Methods	2
Sites	2
Crop Model	2
Inputs	3
Simulations	4
Statistical Analysis and Yield Functions	4
Results and Discussion	5
Comparison of Simulated and Observed Phenology and Yields	5
Potential Yield	5
Nitrogen-water Combinations	6
Statistical Analysis and Yield Functions	6
Conclusions	7
References	9
List of Tables	11
List of Figures	12
Tables 1-11	13
Figures 1-8	20

Abstract

CERES-Wheat, a dynamic process crop growth model is specified and validated for eight sites in the major wheat-growing regions of China. Crop model results are then used to test functional forms for yield response to nitrogen fertilizer, irrigation water, temperature, and precipitation. The resulting functions are designed to be used in a linked biophysical-economic model of land-use and land-cover change. Variables explaining a significant proportion of simulated yield variance are nitrogen, irrigation water, and precipitation; temperature was not a significant component of yield variation within the range of observed year-to-year variability except at the warmest site. The Mitscherlich-Baule function is found to be more appropriate than the quadratic function at most sites. Crop model simulations with a generic soil with median characteristics of the eight sites were compared to simulations with site-specific soils, providing an initial test of the sensitivity of the functional forms to soil specification. The use of the generic soil does not affect the results significantly; thus, the functions may be considered representative of agriculturally productive regions with similar climate in China under intensifying management conditions.

Acknowledgments

This research is part of the International Institute for Applied Systems Analysis (IIASA) project "Modeling Land-Use and Land-Cover changes in Europe and Northern Asia".

About the Authors

Cynthia Rosenzweig
Columbia University
NASA/Goddard Institute for Space Studies
2880 Broadway
New York, NY, 10025, USA
Tel: +1-212-678562
Email: cccer@cheops.giss.nasa.gov

Dr. Cynthia Rosenzweig is a Research Scientist at the National Aeronautic and Space Administration (NASA) Goddard Institute for Space Studies, Adjunct Research Scientist at the Columbia Earth Institute, and a member of the IIASA LUC Project. Dr. Rosenzweig's research focuses on the impacts of environmental change, including global warming and El Nino events, on agriculture. She is the co-author with Daniel Hillel of the new book, "Climate Change and the Global Harvest", published in 1998 by Oxford University Press.

Ana Iglesias
Fundacion Premio Arce
Escuela Tecnica Superior de Ingenieros Agronomos
Universidad Politecnica de Madrid
Ciudad Universitaria
28040 Madrid, Spain
Tel: +34-91-3365832
Email: iglesias@ppr.etsia.upm.es

Dr. Ana Iglesias is a Research Scientist at the Polytechnical University of Madrid and at the Center for Climate Systems Research of Columbia University. Dr. Iglesias's research focuses on the impacts of climate change and climatic variability on agriculture, with special emphasis on irrigation. She is a member of the EU-funded projects CLIVARA and concerted action CLAUDE, and since 1995 has contributed to the IIASA project on *Modeling Land-Use and Land-Cover Changes in Europe and Northern Asia*.

Günther Fischer
Leader, Land Use Change Project
International Institute for Applied Systems Analysis
Schlossplatz 1
A-2361 Laxenburg, Austria
Tel: +43-2236-807-292
E-mail: fisher@iiasa.ac.at

Günther Fischer is the leader of a major research project at IIASA on *Modeling Land Use and Land Cover Changes in Europe and Northern Asia (LUC)*. A primary research objective of this project is the development of a GIS-based modelling framework, which combines economic theory and advanced mathematical methods with biophysical land evaluation approaches to model spatial and dynamic aspects of land-resources use. He was a member of the IGBP-HDP Core Project Planning Committee on Land-Use and Land-Cover Change (LUCC), and is a co-author of the LUCC Science Plan. He serves on the Scientific Steering Committee of the joint LUCC Core Project/Programme of the IGBP-IHDP, and leads the *LUCC Focus 3 office* at IIASA.

Yanhua Liu
Deputy Director-General
Bureau of Societal Development
The State Commission of Science and Technology
Fuxingmen Wai Road
Beijing, China
Tel: +8610 649-13-841
E-mail: liuyh@acca21.edu.cn

Professor Yanhua Liu is the Deputy Director-General, Bureau of Societal Development, State Science and Technology Commission, and Professor of Geography at the Institute of Geography, Chinese Academy of Sciences, where he was formerly director from 1995 to 1997. Professor Liu's research activities and responsibilities include: research designs on disaster reduction at state and regional levels; regional planning for economic development in China; program leader for Study Programs; national co-ordinator for the ICIMOD Programs in China; member of the Core Project Planning Committee, Land-Use and Land-Cover Change, IGBP - IHDP; consultant for UNDP & UNEP programs on disaster reduction and RS/GIS, and member of the steering committee of the IIASA project on Modeling Land-Use and Land-Cover Changes in Europe and Northern Asia.

Walter E. Baethgen,
IFDC - Uruguay
J. Barrios Amorin 870 P.3
Montevideo 11200, Uruguay
Tel: +-598-2-711-7817
Email: baethgen+AEA-undp.org.uy;

Dr. Walter Baethgen has a background in crop and soil environmental sciences and coordinates the International Fertilizer Development Center's (IFDC) research and development activities in SE South America. Since 1990 he has been conducting research and development projects mainly in Latin America but also in the USA, Europe and Africa. Recently, Dr. Baethgen has been developing and implementing Information and Decision Support Systems for the agricultural sector of different countries using simulation models and remote sensing. He has also been collaborating with NASA and NOAA for studying the impact of climate variability (seasonal/interannual, and long-term) in the agricultural sector of South America, Asia and the USA.

James W. Jones
Agricultural and Biological Engineering Department
University of Florida
Gainesville, FL 32611, USA
Tel: + 1-352-392-8694
Email: jwj@agen.ufl.edu

Dr. James Jones is a Distinguished Professor at the Agricultural and Biological Engineering Department, University of Florida, and has over 25 years experience in agricultural systems analysis. Much of his work has focused on development of crop simulation models for general use and on decision support systems for application of these models to a wide range of research and practical issues. He has considerable experience in research on relationships between weather and crop growth, and has applied this expertise in research on impacts of climate change on agriculture and on potential for agricultural uses of seasonal to annual climate predictions.

Wheat Yield Functions for Analysis of Land-Use Change in China

Cynthia Rosenzweig, Ana Iglesias, Günther Fischer, Yanhua Liu, Walter Baethgen, and James W. Jones.

INTRODUCTION

China is undergoing rapid changes in economic structure and development, urban and rural lifestyles, demands on land and water resources, and pressures on the environment. Its population is predicted to continue to grow for at least another 30 years, and to reach a population level of about 1.4-1.5 billion people by the year 2030 (Fischer and Heilig, 1997). Recognizing the need to project China's likely course of agricultural development, the International Institute for Applied Systems Analysis (IIASA) Land-Use and Land-Cover Change (LUC) Project is assembling a set of databases and analytical tools (IIASA, 1998; Fischer et al., 1997). These tools combine biophysical understanding of agro-ecosystem processes (Rosenzweig and Iglesias, 1998), a compilation of land and water resources, and a multi-regional, multi-sectoral dynamic economic model of China's food economy.

Wheat is currently grown in many regions of China with productivity levels that depend greatly on management inputs. Here we utilize a calibrated and validated dynamic process crop growth model, CERES-Wheat (Ritchie and Otter, 1985), and data from the IIASA-LUC geographic information system (GIS) to test site-based crop responses to management, specifically nitrogen fertilizer and water for irrigation, for the observed range of interannual climate variability.

A variety of functional forms have been tested for the response of crop yields to inputs (e.g., Franke et al., 1990). We test two regression models utilizing simulated crop yield responses as possible yield functions for the economic model: the quadratic and the Mitscherlich-Baule. The quadratic function tested imposes non-zero elasticity of substitution among factors and diminishing marginal productivity:

$$Y_i = \alpha_1 + \alpha_2 (N_i) + \alpha_3 (W_i) + \alpha_4 (N_i)^2 + \alpha_5 (W_i)^2 + \alpha_6 (N_i W_i)$$

where Y_i is wheat yield (kg ha^{-1}), N_i is nitrogen applied (kg ha^{-1}), W_i is water amount (mm), and α_{1-6} are parameters.

The Mitscherlich-Baule function has been found to be preferable for use in an economic model, because it allows for factor substitution and a growth plateau following von Liebig's "Law of the Minimum" (Llewelyn and Featherstone, 1997). The Mitscherlich-Baule function is of the form:

$$Y_i = \beta_1 * (1 - \exp(-\beta_2 (\beta_3 + N_i))) * (1 - \exp(-\beta_4 (\beta_5 + W_i)))$$

where Y_i is wheat yield (kg ha^{-1}), N_i is nitrogen applied (kg ha^{-1}), W_i is water amount (mm), and β_{1-5} are parameters. β_1 represents an asymptotic yield level plateau, β_3 and β_5 can be interpreted as the residual levels of nitrogen and water in the soil.

The objective of this study is to determine the variables that explain a significant proportion of simulated yield variance across the major wheat-growing region of China and to specify appropriate functional forms for use in the linked IIASA-LUC biophysical-economic model of land-use and land-cover change. The crop model is used because experimental agronomic data are lacking across the large area where wheat is grown. The crop models further provide testable results at sites for the more spatially generalized scale used in the land-use change model.

METHODS

Sites

CERES-Wheat is calibrated and validated across eight sites spanning the wheat-growing regions of China (Fig. 1 and Table 1). The sites represent the climate conditions under which wheat is grown in China, ranging from the continental climate of the traditional wheat-growing regions in the North China Plain (Beijing and Liaocheng) to the moderately warm subtropical zone in the center of the country (Chengdu). Yulin represents the marginal desert-transition zone of the loess plateau; Xi'an lies in the central reaches of the Yellow River basin; and Xuzhou, Suzhou and Nanjing are found in the fertile plain of the Yangtze River. Winter wheat is grown in the cooler areas; in the warmer areas, spring wheat is sown in the late fall and matures without vernalization. Both rainfed and irrigated wheat areas are represented, as specified by the IIASA-LUC county-level data.

Crop Model

Yield responses to climate and management were simulated with CERES-Wheat (Ritchie and Otter, 1985; Ritchie et al., 1988; Godwin et al., 1990), a process-based mechanistic model that simulates daily phenological development and growth in response to environmental factors (soil and climate) and management (crop variety, planting conditions, nitrogen fertilization, and irrigation). The model is designed to have applicability in diverse environments and to utilize a minimum data set of commonly available field and weather data as inputs. CERES-Wheat has been calibrated and validated over a wide range of agro-climatic regions (see, e.g., Rosenzweig and Iglesias, 1998).

Nitrogen dynamics in the model include mineralization and/or immobilization of N associated with the decay of crop residues, nitrification, denitrification, urea hydrolysis, leaching of nitrate, and the uptake and use of N by the crop (Godwin and Jones, 1991). The N model uses the layered soil-water balance model described by Ritchie (1985) and the soil temperature component of the EPIC model (Williams et al., 1983). The nitrogen formulation in CERES-Wheat has also been tested in diverse environments (see, e.g., Kovacs et al., 1995; Semenov et al., 1996).

Inputs

Climate. Daily climate variables (maximum and minimum temperature and precipitation) for the eight sites were provided by Dr. Roy Jenne of the U.S. National Center for Atmospheric Research. Time-series for the different sites ranged from 15 to 30 years. Daily solar radiation for each time-series was generated using the WGEN weather generator (Richardson and Wright, 1984).

Figure 2 shows average monthly temperature and precipitation for the sites and Table 1 shows the length of record, the average annual temperature and precipitation, and the growing period precipitation (defined as days between simulated sowing and maturity). The wheat growing period corresponds to the dry period of the year at all sites. In general, this period also shows large interannual variability. At the drier sites (Beijing, Yulin, and Liaocheng), the growing season precipitation is less than 200 mm and its coefficient of variation varies from 21 to 55%, implying risk of dryland crop failures and the need for supplemental irrigation to meet crop water requirements.

Soil. Characteristics of the soil at each site needed as crop model inputs include albedo and runoff curve number. For each soil layer, inputs include depth; texture; water-holding capacity at drained lower and upper limits, and at saturation; bulk density; pH; and organic carbon. These characteristics were specified for the crop model simulations at each site based on Jin et al. (1995 and personal communication), the Chinese Soil Taxonomic Classification System (1991), ISSAS and ISRIC (1995), and Zheng et al. (1994) (Table 2). The agricultural soils across the range of sites are primarily sandy and sandy loams of medium depth, with neutral pH and low-to-moderate levels of organic carbon. It is important to note that dynamic process crop growth models such as the one used in this work require layered soil-profile characteristics that are often not specified with adequate detail in currently published global or regional databases.

In addition to the site-specific soils, a generic soil was created by selecting the median value of the soil characteristics over all sites (Table 2). This was done so that crop model simulations with the generic soil could be compared to simulations with the site-specific soils, providing an initial test of the sensitivity of the results to soil specification.

Management Variables. Cultivars, planting dates, and plant population (200 plants m^{-2}) were specified based on current practices and crop cultivar calibration and validation as described by Jin et al. (1995 and personal communication) (Table 3). Nitrogen is assumed to be broadcast as ammonium nitrate before planting (30 kg ha^{-1}), with the remainder applied in the spring. Initial soil ammonium and nitrate concentrations are from the Chinese Academy of Agricultural Sciences. Initial soil water was calculated for each site by running the model for the entire time-series of weather and averaging the soil moisture at planting time. The soil-water component was initiated ten days before sowing date.

Simulations

Three sets of simulations were done:

- 1) **Validation.** The first set of simulations was run with observed soils, cultivars, and management for comparison to observed wheat development stages and yields. For nitrogen and water applications, county-level data for 1989/90 from the IIASA-LUC database for total fertilizer applications (divided by the number of crops per year) and irrigated percentage of crop production were aggregated to prefecture-level. Observed wheat yield data were also aggregated to the prefecture level and represent average wheat yield for all types of production within the administrative unit.
- 2) **Potential yield.** The second set utilized automatic nitrogen and irrigation application according to the specifications shown in Table 4. The results of these simulations provide the yield potential with non-limiting nitrogen and water conditions at each site, given current climate and management conditions. Because system efficiencies are set at 100%, nitrogen and water results for these simulations represent net crop nitrogen demand and net irrigation water demand, not actual amounts applied in the field. These simulations were done both with the site-specific soils and the generic soil.
- 3) **Nitrogen-water combinations.** The third set was comprised of combinations of thirteen levels of nitrogen (0, 15, 30, 45, 60, 75, 90, 105, 120, 135, 150, 180, and 210 kg ha⁻¹) and twenty-one levels of irrigation (from 0 to 600 mm in 30 mm increments). For the irrigation treatments, one irrigation treatment was applied before planting; then, after winter dormancy, equal amounts of irrigation were scheduled at varying time intervals, taking into account the specific time-dependent crop water demand at each site (Fig. 3). Irrigation intervals were longer during the early crop growth stages and shorter in the period from shortly before anthesis up to physiological maturity. This resulted in 4095 to 8190 simulations per site, depending on length of climate time-series. These simulations were also done both with the site-specific soils and the generic soil.

The CERES-Wheat model outputs analyzed were: dates of anthesis and maturity, grain yield, nitrogen fertilizer applied, and irrigation water amount.

Statistical Analysis and Yield Functions

Because of the differences in response to nitrogen and irrigation due to climatic differences across the study sites, we calculated temperature and precipitation anomalies for March, April, May, and June, and precipitation anomalies over the entire growing period for inclusion in the statistical analysis and yield response functions.

The relationships between wheat yield, input variables, and temperature and precipitation anomalies taken singly were first analyzed using the Pearson product moment correlation coefficient calculated by the SPSS statistical program. This exploratory analysis served to identify variables explaining a significant proportion of the observed yield variance.

Then the quadratic and Mitscherlich-Baule regression models were tested as possible yield functions. For each function, the agreement between the simulated “observed” yields (we now use “observed” to designate the results of the CERES-Wheat simulations) and yields predicted by the functions was measured using the adjusted R², representing the fraction of

variation in simulated yield explained by the fitted yield values. We also assessed the significance of the estimated models by screening the values obtained for the F-test. F values were less than 0.0001 at the 95% significance level. Function parameters, their significance, and predicted yields were calculated using the SPSS statistical program.

RESULTS AND DISCUSSION

Comparison of Simulated and Observed Phenology and Yields

Table 5 shows a comparison of simulated and observed dates of sowing, anthesis and maturity for wheat at the eight sites. The selected sowing dates and observed phenology were derived from information published by the USDA Foreign Agricultural Service (FAS, 1997). In general, the crop model simulates anthesis and crop maturity somewhat earlier than observations. The crop model defines anthesis as the date when 50% of the crop is shedding pollen and physiological maturity as the day that grain-filling ends; observations in the field for these two stages are often made slightly later. However, since wheat crop nitrogen and water requirements in the latter part of the phenological cycle are usually small, the discrepancy in maturity dates is not likely to affect the use of the model to determine nitrogen and water response functions.

Table 6 shows the fertilizer and irrigation management used in the validation simulations and comparisons of observed and simulated wheat yields. Reported fertilizer applications and percent of crop production that is irrigated for the prefecture in which the sites are located are used to derive the input values used in the CERES-Wheat simulations. The high reported fertilizer applications at some sites were reduced to take account of multiple crops per year. Similarly, since the high reported irrigation percentage in Xi'an, Nanjing, Suzhou, Xuzhou, and Chengdu reflects the use of irrigation for all crops (especially rice), we set the irrigation percentage for the validation simulations for these sites at 50%. Simulated yields are generally higher than observed yields, but represent reported yields fairly well. The models do not consider limitations due to nutrients other than nitrogen, nor possible yield reductions caused by weeds, pests and diseases, and flooding; thus crop model simulations are usually taken to represent an upper limit of crop production for the management systems and sites tested.

Potential Yield

Table 7 shows modeled wheat yields, nitrogen applications, and irrigation amount under non-limiting nitrogen and water regimes. Potential yields give an indication of the maximum yield possible under current climate and management conditions and are fairly similar across the transect of sites. Nitrogen applications are related to the initial fertility levels of the sites (Liaocheng and Suzhou), and water applications are highest in the dry sites (Beijing, Yulin, and Liaocheng).

At high levels of inputs as represented by these simulations, differences between the site-specific soils and the generic soil have minor effects on potential yield, simulated nitrogen fertilizer applied, and irrigation amount. The effect on yields of using a generic soil rather than a site-specific soil was within 5%. This result indicates, in part, that intensive management can overcome non-optimal soils. The comparison between the two soils also provides an initial test of the sensitivity of the simulation results described in the next section to soil specification.

Nitrogen-water Combinations

Figure 4 shows the effect of nitrogen fertilizer and irrigation on simulated wheat yields at Liaocheng, a dry site, and Nanjing, a well-watered site. The points represent the simulated yield values for each year. At both wet and dry sites, the variation of yield for a particular nitrogen level is smaller if the crop is well-watered and larger in dryland settings. Across nitrogen levels, more benefit is found to fertilizer application in irrigated rather than dryland crops, since nutrient uptake is limited under dry conditions. The dry site displays lower response to nitrogen and lower yields; the greatest response is seen at the dry site when irrigation is applied at high nitrogen fertilization.

Crop responses at Beijing and Yulin are similar to the one at Liaocheng; those at Chengdu and Suzhou are similar to that of Nanjing; responses at Xi'an and Xuzhou are intermediate. At Chengdu, the response to nitrogen fertilizer is very similar in dryland and irrigated simulations because of the high precipitation regime.

Statistical Analysis and Yield Functions

Correlation coefficients. Table 8a shows the correlation coefficients at the eight sites between wheat yields, inputs (nitrogen and water) and variations in temperature and precipitation in the observed climate record. Climate anomalies are for March to June when the crop is actively growing. As expected, yields at drier sites are less well-correlated with nitrogen fertilizer applications than yields at wetter sites; yields at drier sites are, of course, highly correlated with irrigation amounts. Yields at the different sites respond differently to precipitation anomalies in the individual months of the growing period, due to differences in crop-climate interactions. In general, however, yields are correlated with precipitation anomalies over the growing period. Temperature anomalies from March to June generally have a smaller and mostly negative effect on yields.

Table 8b shows correlations of non water-limited yields with nitrogen fertilizer applications and temperature anomalies in March, April, May, and June. Non water-limited wheat yields are highly correlated with nitrogen fertilizer levels at all sites. As with the yields in the nitrogen-water combinations, the effects of temperature anomalies during March through April on yields in the non-limiting water simulations are generally small.

From this analysis, it appears that nitrogen fertilization level, irrigation amount, and precipitation anomalies are important variables to include in the functional forms for these sites, but that temperature anomalies in the range of climates tested are less important in explaining yield variation. Under warming conditions due to the enhanced greenhouse effect, these results may not hold (Rosenzweig and Hillel, 1998).

An example of the relationships of simulated wheat yield to temperature and precipitation anomalies is shown in Figure 5. Dryland yields at Chengdu, a warm site, are negatively correlated to temperature at anthesis over the range of observed anomalies; they are also negatively correlated to decreases in growing season precipitation. In contrast, irrigated yields at Chengdu are correlated to neither of these observed anomalies.

Yield response functions. An example of the yield data from the crop model simulations is shown in Table 9 for Liaocheng; each value is the average of crop model simulations for the years of climate record (in this case, 16 years of climate record). At higher input levels (nitrogen applied greater than 120 kg ha⁻¹ and irrigation more than 400 mm), a

yield plateau of approximately 5500 kg ha⁻¹ was reached, representing the biophysical crop yield limit given the specified management conditions. Similar data for each site were used to test the quadratic and Mitscherlich-Baule functional forms.

The quadratic and Mitscherlich-Baule functional forms were tested with the inclusion of management inputs (nitrogen fertilizer and irrigation water amounts); then functions including temperature and/or precipitation anomalies during the growing season were tested. Precipitation anomalies were added to the irrigation water term, providing a term representing the overall water status of the crop during the growing season. At all sites, the incorporation of temperature anomalies in the functions did not improve the adjustment between observed and predicted yields, and the function parameters in the temperature terms were not significant.

Figures 6 and 7 show CERES-Wheat simulated yields and predicted yields with different specifications of quadratic and Mitscherlich-Baule functions at Beijing. Quadratic 1 and Mitscherlich-Baule 1 are the functions with management inputs alone; Quadratic 2 and Mitscherlich-Baule 2 include precipitation anomalies. The inclusion of precipitation anomalies in the water term allows for calculation of the effects of year-to-year variation in climate, a useful attribute that allows for consideration of risk in the economic model. Return to inputs is better represented in the Mitscherlich-Baule functions. Table 10 shows the adjusted R² values obtained with the Quadratic 2 and the Mitscherlich-Baule 2 forms. Table 11 shows the parameters in the functional forms (all significant at the 95 percent level); the Mitscherlich-Baule parameters are more stable than those of the quadratic function.. Figure 8 shows a comparison of observed and predicted yields for the site-specific soils with the Mitscherlich-Baule 2 function that includes the precipitation variation.

When using the Mitscherlich-Baule function in the context of an optimizing economic model, it is important to note that specifications with more than one input factor (e.g., nutrients and water) exhibits increasing returns to scale. To ensure constant returns to scale, a generalized form of the Mitscherlich-Baule function should be applied:

$$Y_i = \beta_1 * (1 - \exp(-\beta_2 (\beta_3 + N_i)))^{\theta_1} * (1 - \exp(-\beta_4 (\beta_5 + W_i)))^{\theta_2}$$

In this example, the returns to scale is controlled by the sum $\theta_1 + \theta_2$, and constant returns to scale is achieved with setting $\theta_1 + \theta_2 = 1$.

The adjusted R² values are not very sensitive to the use of the generic soil with median characteristics across the main wheat region of China (Tables 10 and 11). Thus, the functions may be considered representative of agriculturally productive regions with similar climate in China under intensifying management conditions. Variation in soil characteristics is more important at lower levels of nitrogen and water inputs than at higher levels.

CONCLUSIONS

This work links biophysical and economic models in a rigorous and testable methodology. The validated crop model is useful for simulating the range of conditions under which wheat is grown in China, and provides the means to estimate production functions when experimental field data are not available. The Mitscherlich-Baule functional form does appear to be more useful than the quadratic form for a land-use change model due to its simulation of the growth plateau and input substitutability. Understanding the role of soil characteristics in the crop response functions helps to validate the use of site-based results over the larger geographic regions of the economic model.

Further work will involve developing scaling techniques to utilize the estimated functions for wheat throughout the current agricultural region of China. Expanding the range of their applicability in regard to higher temperature, changed hydrological regimes, higher levels of atmospheric carbon dioxide, and sulfate aerosols will allow for the use of the work for global environmental change projections.

References

- Fischer, G. Y. Ermoliev, M.A. Keyzer, and C. Rosenzweig. 1996. *Simulating the Socio-economic and Biogeophysical Driving Forces of Land-use and Land-cover Change: The IIASA Land-use Change Model*. IIASA Working Paper. WP-96-010. 83 pp.
- Fischer, G. and G.K. Heilig. 1997. Population momentum and the demand on land and water resources. *Phil. Trans. R. Soc. Land. B* (1997) 352:869-889
- Franke, M.D., B.R. Beattie, M.F. Embleton. 1990. A comparison of alternative crop response models. *American Journal of Agricultural Economics* 72:597-602.
- Godwin, D.C. and C. A. Jones. 1991. Nitrogen dynamics in soil-plant systems. In J. Hanks and J.T. Ritchie (eds.). *Modeling Plant and Soil Systems*. American Society of Agronomy. Agronomy Series No. 31. pp. 287-321.
- Godwin, D., J. Ritchie, U. Singh, and L. Hunt. 1990. *A Users Guide to CERES Wheat, version 2.10*. International Fertilizer Development Center. Muscle Shoals, AL. 94 pp.
- FAS. 1997. Foreign Agricultural Service of the US Department of Agriculture.
- IIASA. 1998. iiasa.ac.at/Research/LUC/GIS/giswebpage. May 18, 1998.
- CSTCS. 1991. Chinese Soil Taxonomic Classification System. In: ISSAS & ISRIC. 1995. *Reference Soil Profiles of the People's Republic of China: Field and Analytical Data*. Institute of Soil Sciences. Academia Sinica and International Soil Reference and Information Centre. Wageningen, The Netherlands.
- Jin, Z., D. Ge., H. Chen, and J. Fang. 1995. Effects of climate change on rice production and strategies for adaptation in southern China. In C. Rosenzweig, L.H. Allen, Jr., L.A. Harper, S.E. Hollinger, and J.W. Jones (eds.). *Climate Change and Agriculture: Analysis of Potential International Impacts*. American Society of Agronomy. Special Publication No. 59. Madison, WI. pp. 307-323.
- Kovacs, G.J., T. Nemeth, and J.T. Ritchie. 1995. Testing simulation models for the assessment of crop production and nitrate leaching in Hungary. *Agricultural Systems* 49:385-397.
- Llewelyn, R.V. and A.M. Featherstone. 1997. A comparison of crop production functions using simulated data for irrigated corn in western Kansas. *Agricultural Systems*.
- Richardson, C.W. and D.A. Wright. 1984. *WGEN: A Model for Generating Daily Weather Variables*. ARS-8. U.S. Department of Agriculture. Agricultural Research Service. Washington, DC. 83 pp.
- Ritchie, J.T. 1985. A user-oriented model of the soil water balance in wheat. In W. Day and R.K. Atkin (ed.). *Wheat Growth and Modelling*. Plenum Publ. Corp. New York. pp. 293-306.

- Ritchie, J.T. and S. Otter. 1985. *Description and performance of CERES-Wheat: A user-oriented wheat yield model*. In W.O. Willis (ed.). ARS Wheat Yield Project. U.S. Dept. of Agriculture, Agricultural Research Service. ARS-38. Washington, DC. pp. 159-175.
- Ritchie, J.T., D.C. Godwin, and S. Otter-Nacke. 1988. *CERES-Wheat. A Simulation Model of Wheat Growth and Development*. Texas A&M University Press. College Station, TX.
- Rosenzweig, C. and D. Hillel. 1998. *Climate Change and the Global Harvest: Potential Impacts of the Greenhouse Effect on Agriculture*. Oxford University Press. New York. 336 pp.
- Rosenzweig, C. and A. Iglesias. 1998. The use of crop models for international climate change impact assessment. In Tsuji, G.Y., G. Hoogenboom, and P.K. Thornton (eds.). *Understanding Options for Agricultural Production*. Kluwer Academic Publishers. Dordrecht. pp. 267-292.
- Semenov, M.A., J. Wolf, L.G. Evans, H. Ackersten, and A. Iglesias. 1996. Comparison of wheat simulation models under climate change. *Climate Research* 7:271-181.
- Williams, J.R., P.T. Dyke, and C.A. Jones. 1983. EPIC -- A model for assessing the effects of erosion on soil productivity. In W.K. Lavenroth et al. (ed.). *Proc. Third Int. Conf. on State-of-the-Art in Ecological Modelling*. Fort Collins, CO. 24-28 May 1982. Elsevier Sci. Publ. Co., New York.
- Zheng, Z., X. Liu, Z. Meng, and D. Zheng. 1994. *Land Utilization Types in China*. United Nations Development Program; State Science and Technology Commission of the People's Republic of China; Food and Agriculture Organization of the United Nations; State Land Administration of the People's Republic of China. Beijing. 144 pp.

Tables

Table 1. Site, province, latitude and longitude, length of daily climate record, mean annual temperature and precipitation, and mean wheat growing-period precipitation at crop-modeling sites.

Table 2. Soil inputs for crop model simulations.

Table 3. Planting date, wheat cultivars, and genetic coefficients (Jin et al., 1995).

Table 4. Automatic management of non-limiting nitrogen and water conditions.

Table 5. Observed and simulated dates of sowing, anthesis and maturity for wheat.

Table 6. Yield validation simulations and results.

Table 7. Simulated wheat yield, nitrogen fertilizer applied and irrigation amount.

Table 8. Correlation coefficients between wheat yield and management inputs (nitrogen fertilizer and irrigation amounts) and current observed climate anomalies (temperature and precipitation).

Table 9. Simulated wheat yield response to nitrogen and irrigation in Liaocheng.

Table 10. Adjusted R^2 values of the predicted yields with the Quadratic 2 and Mitscherlich-Baule 2 regression models.

$$\text{Quadratic 2: } Y_i = \alpha_1 + \alpha_2(N_i) + \alpha_3(I_i) + \alpha_4(N_i)^2 + \alpha_5(W_i)^2 + \alpha_6(N_i(I_i + P_i))$$

$$\text{Mitscherlich-Baule 2: } Y_i = \beta_1 * (1 - \exp(-\beta_2(\beta_3 + N_i))) * (1 - \exp(-\beta_4(\beta_5 + (I_i + P_i))))$$

Table 11. Estimated coefficients in the Quadratic 2 and Mitscherlich-Baule 2 model.

Figures

- Figure 1. Wheat growing areas and study sites in China.
- Figure 2. Observed temperature and precipitation at the study sites.
- Figure 3. Irrigation water demand with optimal nitrogen fertilization at each site.
- Figure 4. Effect of nitrogen fertilizer and irrigation on wheat yields at Liaocheng and Nanjing. Yield (I=0): Yield with 0 mm supplemental irrigation; Yield (I=420): Yield with 420 mm supplemental irrigation (optimal irrigation level); Yield (N=0): Yield with 0 kg ha⁻¹ of nitrogen fertilizer; Yield (N=180): Yield with 180 kg ha⁻¹ of nitrogen fertilizer (optimal fertilization level).
- Figure 5. Effect of variation in the observed temperature during the anthesis period (month 5) and growing precipitation on simulated dryland and fully irrigated wheat yields at Chengdu.
- Figure 6. CERES-Wheat and predicted yields with Quadratic non-linear regression models at Beijing.
- Figure 7. CERES-Wheat and predicted yields with Mitscherlich-Baule models at Beijing.
- Figure 8. Comparison of yields simulated with the CERES-Wheat model and predicted with the Mitscherlich-Baule 2 model.

Table 1. Site, province, latitude and longitude, length of daily climate record, mean annual temperature and precipitation, and mean wheat growing-period precipitation at crop-modeling sites.

Site	Province	Lat. ⁽¹⁾	Long. ⁽¹⁾	Years ⁽²⁾	Temp. (° C)	Prec (SD) (mm)	GP ⁽³⁾ Prec (SD) (mm)
Beijing	Beijing	39.97	116.32	58-77	12.6	636 (258)	152 (84)
Liaocheng	Shandong	36.02	115.35	79-95	14.1	482 (126)	178 (68)
Yulin	Shaanxi	38.14	109.42	79-95	9.7	324 (86)	169 (68)
Xi'an	Shaanxi	34.25	108.90	59-87	14.4	546 (118)	275 (58)
Nanjing	Jiangsu	32.00	118.80	59-89	15.9	1016 (198)	478 (102)
Suzhou	Jiangsu	31.16	120.37	79-95	16.0	971 (387)	504 (164)
Xuzhou	Jiangsu	34.32	117.37	51-80	14.6	869 (200)	307 (111)
Chengdu	Sichuan	30.67	104.07	58-77	16.7	977 (210)	185 (56)

⁽¹⁾ Latitude north and longitude east in degrees and decimals.

⁽²⁾ Length of daily climate record.

⁽³⁾ Growing period is time between sowing and maturity.

Table 2. Soil inputs for crop model simulations.

Site	CSTCS Soil Group	Depth (cm)	Texture	Top 30 cm soil layer					
				Water content			Bulk density	pH	Organic carbon (%)
				Lower limit (vol %)	Drained upper limit (vol %)	Saturation (vol %)			
Beijing	Cinnamon	87	Sandy	7.1	19.7	47.5	1.25	8.3	1.47
Liaocheng	Yellow brown	124	Sandy-clay	8.3	21.0	42.3	1.32	8.3	0.52
Yulin	Yellow brown	75	Sandy	9.8	21.6	46.5	1.20	8.1	0.52
Xi'an	Heilu soil	115	Sandy	2.1	15.4	44.9	1.25	7.9	0.80
Nanjing	Yellow brown	75	Sandy-loam	9.8	21.6	46.5	1.20	6.5	1.70
Suzhou	Yellow brown	124	Sandy-clay	8.3	21.0	42.3	1.32	6.4	1.80
Xuzhou	Yellow brown	100	Sandy	2.6	12.2	34.6	1.59	8.3	0.53
Chengdu	Purple	110	Silt-loam	16.5	29.6	34.9	1.50	6.5	1.07
All sites	Generic soil	96	Sandy-loam	8.3	20.0	42.7	1.32	7.0	1.50

Sources: Chinese Soil Taxonomic Classification System, (CSTCS, 1991. *In*: ISSAS & ISRIC (1995)); Zheng *et al.* (1994).

Table 3. Planting date, wheat cultivars, and genetic coefficients (Jin et al., 1995).

	Planting date	Cultivar ⁽¹⁾						
		Name	P1V	P1D	P5	G1	G2	G3
Beijing								
Liaocheng	29 Sept	F.K. 2	4.0	3.8	2.4	3.5	4.3	3.0
Yulin								
Xi'an	10 Oct	Y.M. 2	6.5	4.2	5.5	5.5	5.5	3.0
Nanjing	25 Oct	Yanmai 5	6.0	4.0	2.0	5.5	5.0	2.0
Suzhou								
Xuzhou	10 Oct	Jinan 13	4.0	4.8	4.0	4.5	4.2	2.0
Chengdu	2 Nov	M.Y. 11	2.4	4.4	5.0	7.3	4.8	5.0

⁽¹⁾ Genetic coefficients that describe wheat cultivars in the CERES-Wheat model: P1V, vernalization; P1D, photoperiod; P5, grain-filling duration; G1 to G3, grain-filling coefficients. The phylochron interval (the interval in thermal time (degree days) between successive leaf tip appearances) coefficient for all cultivars was 75.

Table 4. Automatic management of non-limiting nitrogen and water conditions.

Automatic management		
Irrigation	Management depth	50 cm
	Threshold	80% of maximum available water in soil
	End point of applications	100% of maximum available water in soil
	Applications	all growth stages
	Method	pressure
	Amount per irrigation	10 mm
	Irrigation efficiency	100%
Nitrogen fertilization	Application depth	15 cm
	Threshold	when crop shows 20% nitrogen stress
	Amount per application	10 kg ha ⁻¹
	Material	ammonium nitrate
	Applications	all growth stages

Table 5. Observed and simulated dates of sowing, anthesis and maturity for wheat.

Site	Planting date		Anthesis date		Maturity date	
	Selected for simulations	Observed	Simulated	Observed	Simulated	Observed
Beijing	29 Sept	15 Sept-15 Oct	23 May	15 May-15 Jun	22 Jun	1-15 July
Liaocheng	29 Sept	15 Sept-15 Oct	16 May	15 May-15 Jun	15 Jun	1-15 July
Yulin	29 Sept	15 Sept-15 Oct	02 Jun	15 May-15 Jun	04 July	1-15 July
Xi'an	10 Oct	15 Sept-15 Oct	18 May	15 May-15 Jun	19 Jun	15-30 Jun
Nanjing	25 Oct	1-31 Oct	14 May	15 May-15 Jun	12 Jun	15-30 Jun
Suzhou	25 Oct	1-31 Oct	15 May	15 May-15 Jun	13 Jun	01-15 Jun
Xuzhou	10 Oct	15 Sept-15 Oct	20 May	15 May-15 Jun	18 Jun	15-30 Jun
Chengdu	2 Nov	15 Oct-15 Nov	22 Apr	1-30 Apr	26 May	01-15 Jun

Source of observations: USDA, FAS (1997). Source of simulations: average of 15 years with management described in Tables 2 and 3.

Table 6. Yield validation simulations and results.

Site	No. of counties	Observations ⁽¹⁾			Simulations ⁽²⁾		
		Total fertilizer sown ha (kg ha ⁻¹)	Share of irrigation (%)	Wheat yield (kg ha ⁻¹)	Nitrogen fertilizer (kg ha ⁻¹)	Wheat irrigation (%)	Wheat yield (kg ha ⁻¹)
Beijing	9	227 (38) ⁽³⁾	81 (1)	4,518 (43)	150 (0)	80 (0)	4,715 (326)
Liaocheng	8	216 (27)	85 (5)	4,546 (388)	150 (0)	80 (0)	4,926 (664)
Yulin	12	27 (20)	12 (13)	454 (370)	30 (0)	10 (0)	578 (649)
Xi'an	7	180 (58)	70 (23)	2,955 (742)	100 (0)	50 (0)	3,533 (534)
Nanjing	6	183 (36)	94 (5)	2,416 (807)	50 (0)	50 (0)	3,511 (560)
Suzhou	7	262 (73)	99 (1)	2,940 (1,853)	75 (0)	50 (0)	3,783 (786)
Xuzhou	7	276 (55)	72 (15)	3,549 (399)	100 (0)	50 (0)	4,108 (975)
Chengdu	13	127 (29)	85 (12)	3,852 (1,410)	75 (0)	50 (0)	4,251 (439)

⁽¹⁾ For nitrogen and water applications, county-level data for 1989/90 from the IIASA-LUC database for total fertilizer applications (divided by the number of crops per year) and irrigated percentage of cultivated land were aggregated to prefecture-level. Observed wheat yield data were also aggregated to the prefecture level and represent average wheat yields for all types of production within the administrative unit.

⁽²⁾ The simulations are the average of the period specified on Table 1 for each site with management shown on Tables 2 and 3. Nitrogen and irrigation simulation inputs were derived from observed values, adjusted for wheat by the characteristics of the cropping system at each site.

⁽³⁾ Average (Standard Deviation).

Table 7. Simulated wheat yield, nitrogen fertilizer applied and irrigation amount.

Site	Site soil			Generic soil		
	Yield (kg ha ⁻¹)	Nitrogen (kg ha ⁻¹)	Irrigation (mm)	Yield (kg ha ⁻¹)	Nitrogen (kg ha ⁻¹)	Irrigation (mm)
Beijing	4,531 (329)	74 (10)	463 (69)	4,412 (428)	91 (57)	427 (72)
Liaocheng	5,216 (405)	141 (48)	443 (56)	5,190 (463)	123 (21)	426 (81)
Yulin	5,237 (256)	67 (10)	402 (38)	4,978 (284)	70 (10)	358 (39)
Xi'an	5,158 (431)	92 (15)	277 (58)	5,077 (457)	108 (18)	271 (57)
Nanjing	4,972 (406)	100 (11)	153 (64)	4,852 (455)	109 (15)	125 (56)
Xuzhou	4,801 (531)	112 (21)	311 (71)	4,764 (522)	94 (17)	276 (75)
Suzhou	5,457 (678)	137 (22)	89 (61)	5,415 (737)	136 (23)	98 (67)
Chengdu	5,240 (373)	57 (7)	136 (40)	5,463 (435)	74 (15)	139 (40)

Table 8. Correlation coefficients between wheat yield and management inputs (nitrogen fertilizer and irrigation amounts) and current observed climate anomalies (temperature and precipitation).

Factor	Correlation coefficients (yield-factor)							
	Beijing	Liaocheng	Yulin	Xi'an	Nanjing	Suzhou	Xuzhou	Chengdu
a) Input (nitrogen and water) limited yield								
Nitrogen	0.08	0.10	0.15	0.32	0.56	0.42	0.17	0.26
Irrig. water	0.73	0.71	0.60	0.39	-0.05	-0.02	0.44	0.18
PA3	0.36	0.50	0.12	-0.02	0.20	0.52	-0.03	0.49
PA4	0.51	-0.02	0.29	0.25	0.39	0.47	0.45	0.56
PA5	0.74	0.64	0.39	0.64	0.34	0.69	0.61	0.21
PA6	0.12	0.16	0.39	0.25	0.28	0.33	-0.15	0.31
PAGP	0.44	0.48	0.59	0.37	0.38	0.78	0.64	0.75
TA3	-0.24	0.11	-0.23	-0.07	-0.09	0.53	0.16	-0.20
TA4	-0.01	-0.30	0.11	0.16	-0.02	0.53	0.14	-0.12
TA5	0.03	-0.31	-0.33	-0.47	-0.42	-0.29	-0.60	-0.54
TA6	-0.06	0.06	-0.41	-0.52	-0.20	-0.07	-0.51	--
a) Water non-limited yield								
Nitrogen	0.86	0.86	0.90	0.84	0.86	0.79	0.79	0.76
TA3	0.03	-0.10	-0.08	0.08	0.08	0.22	0.06	0.01
TA4	0.18	-0.15	0.07	0.07	0.07	0.32	0.16	0.08
TA5	-0.22	-0.25	0.05	-0.04	-0.11	-0.28	-0.24	-0.23
TA6	-0.13	-0.06	-0.20	0.05	0.08	0.07	-0.08	--

PA3-6 = precipitation anomaly of calendar months 3 to 6; PAG = precipitation anomaly during the entire growing period; TA3-6 = temperature anomaly of calendar months 3 to 6.

Table 9. Simulated wheat yield response to nitrogen and irrigation in Liaocheng.

N Fertilizer (kg ha ⁻¹)	Irrigation (mm)										
	0	60	120	180	240	300	360	420	480	540	600
0	930	1287	1627	1913	2170	2364	2481	2514	2502	2462	2374
15	1067	1516	1946	2325	2671	2929	3116	3181	3181	3162	3085
30	1126	1643	2145	2604	3045	3388	3612	3715	3746	3729	3682
45	1150	1725	2299	2807	3313	3742	4015	4163	4199	4184	4137
60	1172	1774	2385	2970	3510	3998	4339	4485	4549	4530	4509
75	1179	1814	2459	3072	3631	4192	4500	4703	4764	4749	4730
90	1199	1837	2508	3155	3731	4311	4674	4866	4951	4933	4929
105	1202	1869	2544	3219	3830	4440	4810	5001	5065	5057	5047
120	1209	1865	2579	3259	3908	4514	4891	5087	5161	5176	5149
135	1213	1882	2615	3320	3972	4604	4967	5141	5247	5245	5240
150	1220	1894	2643	3352	4011	4655	5095	5277	5361	5373	5365
180	1235	1907	2615	3399	4099	4789	5217	5395	5472	5477	5485
210	1238	1904	2635	3426	4148	4840	5270	5476	5551	5547	5566

Table 10. Adjusted R² values of the predicted yields with the Quadratic 2 and Mitscherlich-Baule 2 regression models.

Mitscherlich-Baule 2: $Y_i = \beta_1 * (1 - \exp(-\beta_2 (\beta_3 + Ni))) * (1 - \exp(-\beta_4 (\beta_5 + (Ii + Pi))))$

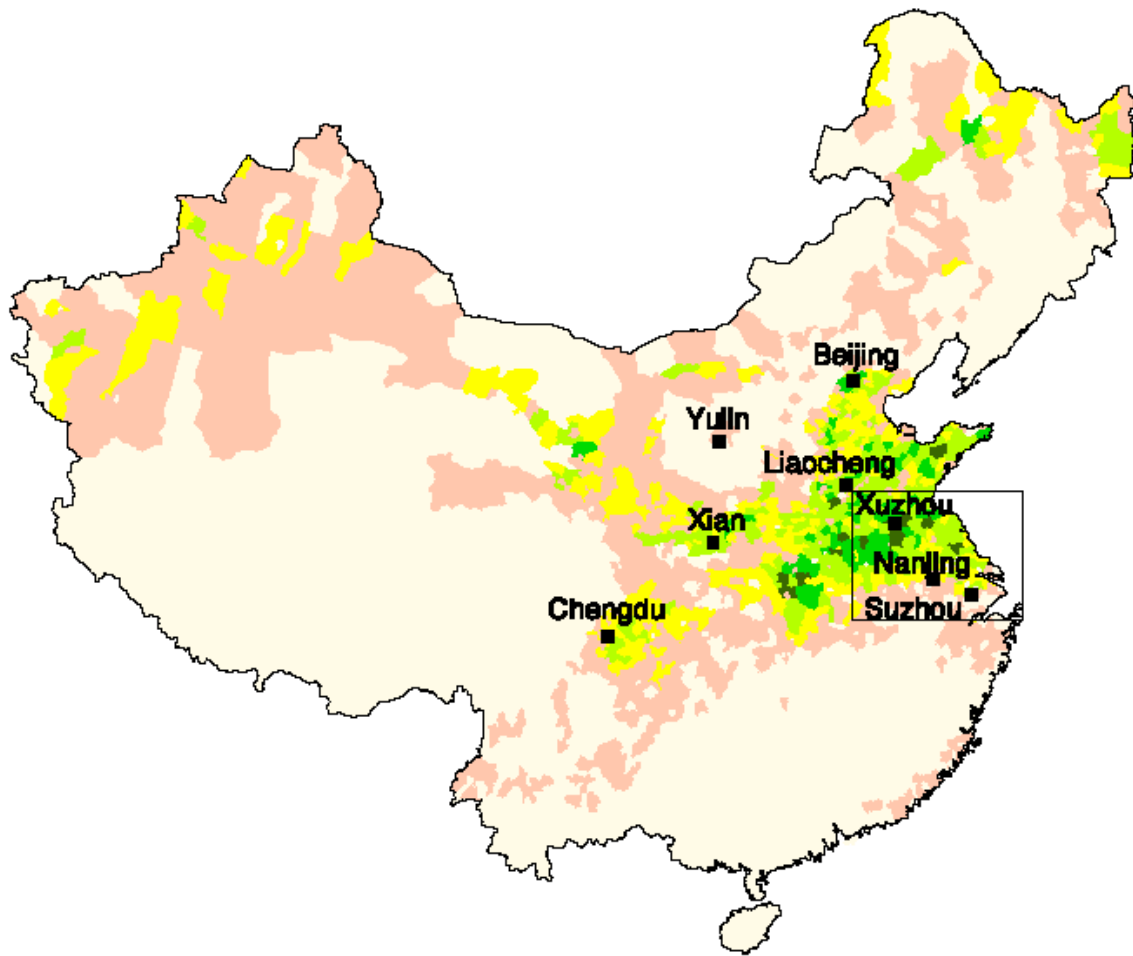
Site	Adjusted R ²			
	Site soil		Generic soil	
	Quadratic	Mitscherlich-Baule	Quadratic	Mitscherlich-Baule
Beijing	0.838	0.839	0.834	0.835
Liaocheng	0.810	0.812	0.805	0.807
Yulin	0.858	0.856	0.867	0.862
Xi'an	0.659	0.668	0.719	0.724
Nanjing	0.564	0.560	0.741	0.728
Suzhou	0.599	0.590	0.539	0.533
Xuzhou	0.544	0.543	0.486	0.496
Chengdu	0.598	0.657	0.623	0.689

All values are significant at the 95% level.

Table 11. Estimated coefficients in the Quadratic 2 and Mitscherlich-Baule 2 model.

SITE	Parameter	Quadratic		Mitscherlich-Baule		
		Site Soil	Generic Soil	Parameter	Site Soil	Generic Soil
Beijing	α_1	101,805	64,81	β_1	6409,01	6266,932
	α_2	10,504	12,201	β_2	0,013	0,013
	α_3	11,146	10,723	β_3	55,569	45,61
	α_4	-0,047	-0,054	β_4	0,003	0,004
	α_5	-0,011	-0,012	β_5	24,9	25,47
	α_6	0,021	0,025			
Liaocheng	α_1	380,117	396,532	β_1	6259,596	6528,261
	α_2	15,46	14,211	β_2	0,018	0,018
	α_3	11,792	10,633	β_3	37,08	36,858
	α_4	-0,066	-0,064	β_4	0,004	0,003
	α_5	-0,013	-0,011	β_5	47,652	52,059
	α_6	0,023	0,025			
Yulin	α_1	251,521	225,207	β_1	6829,595	6671,819
	α_2	14,88	19,874	β_2	0,015	0,014
	α_3	14,596	14,685	β_3	47,317	36,491
	α_4	-0,066	-0,084	β_4	0,004	0,006
	α_5	-0,017	-0,019	β_5	27,354	27,182
	α_6	0,026	0,031			
Xi'an	α_1	1972,621	1450,836	β_1	5863,469	5896,637
	α_2	17,632	21,962	β_2	0,014	0,014
	α_3	10,025	9,543	β_3	63,95	45,825
	α_4	-0,059	-0,074	β_4	0,01	0,009
	α_5	-0,014	-0,014	β_5	72,601	69,597
	α_6	0,011	0,017			
Nanjing	α_1	2989,912	2698,605	β_1	5480,658	5473,28
	α_2	19,09	26,388	β_2	0,013	0,013
	α_3	2,754	0,781	β_3	66,621	43,477
	α_4	-0,059	-0,08	β_4	0,016	0,032
	α_5	-0,005	-0,003	β_5	110,087	79,695
	α_6	0,008	0,01			
Suzhou	α_1	3096,824	2921,747	β_1	5912,683	5919,427
	α_2	26,107	26,016	β_2	0,013	0,013
	α_3	0,407	1,186	β_3	48,799	48,825
	α_4	-0,077	-0,076	β_4	0,045	0,027
	α_5	-0,003	-0,004	β_5	63,229	86,139
	α_6	0,01	0,01			
Xuzhou	α_1	1137,251	1568,308	β_1	5275,731	5390,45
	α_2	19,859	17,203	β_2	0,013	0,015
	α_3	6,934	8,852	β_3	38,33	54,793
	α_4	-0,07	-0,058	β_4	0,007	0,008
	α_5	-0,01	-0,011	β_5	87,214	81,861
	α_6	0,02	0,011			
Chengdu	α_1	3549,224	3234,61	β_1	5801,356	5789,534
	α_2	22,602	24,76	β_2	0,025	0,025
	α_3	4,42	5,006	β_3	43,686	39,562
	α_4	-0,083	-0,092	β_4	0,03	0,026
	α_5	-0,008	-0,008	β_5	45,934	47,277
	α_6	0,007	0,008			

Figure 1. Wheat growing areas and study sites in China.



Case Studies In JIANGSU Province

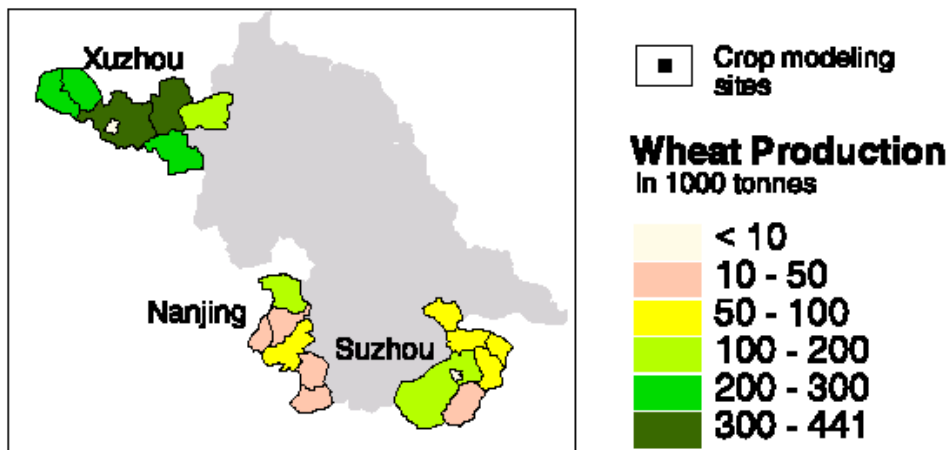


Figure 2. Observed temperature and precipitation at the study sites.

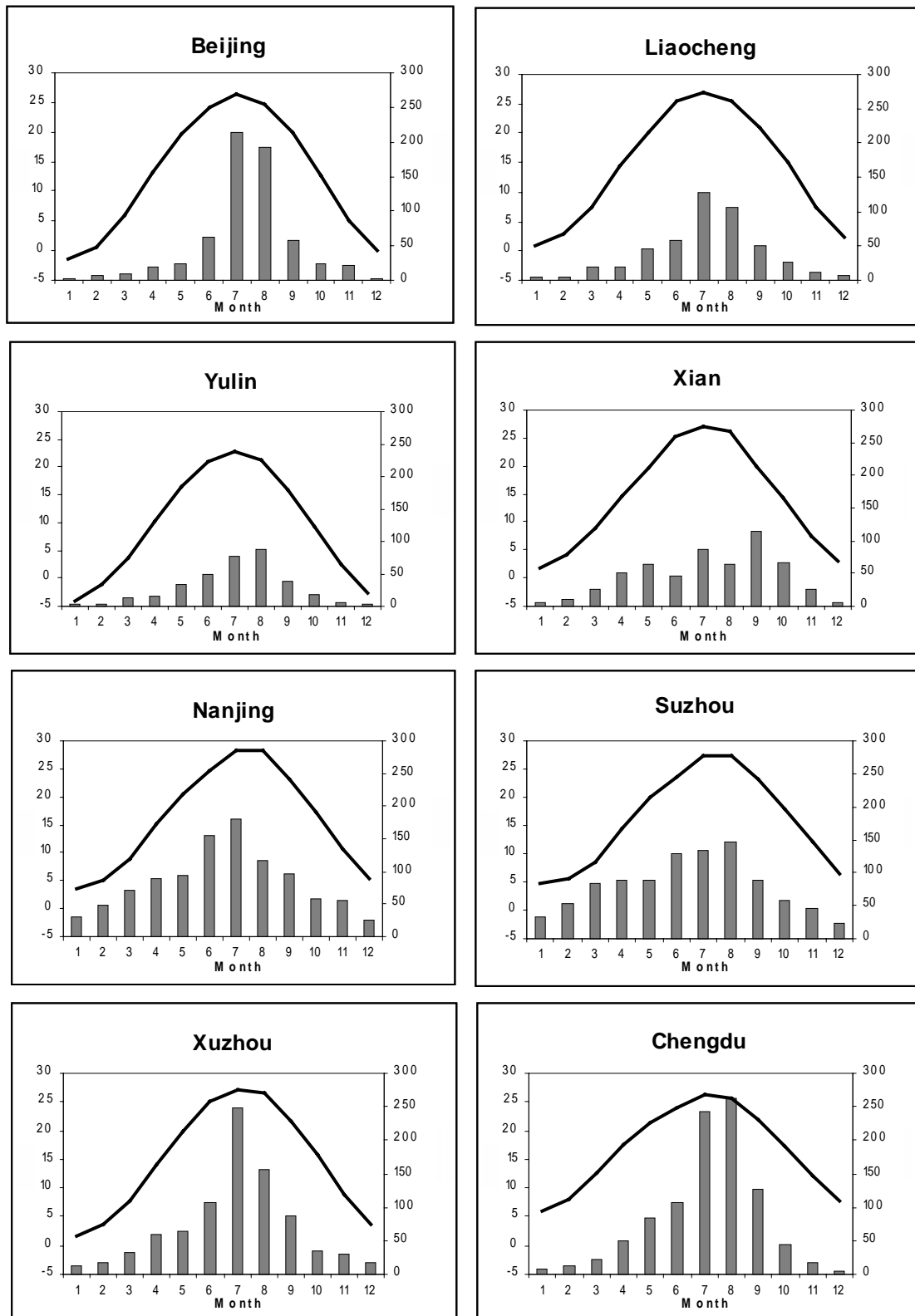


Figure 3. Irrigation water demand with optimal nitrogen fertilization at each site.

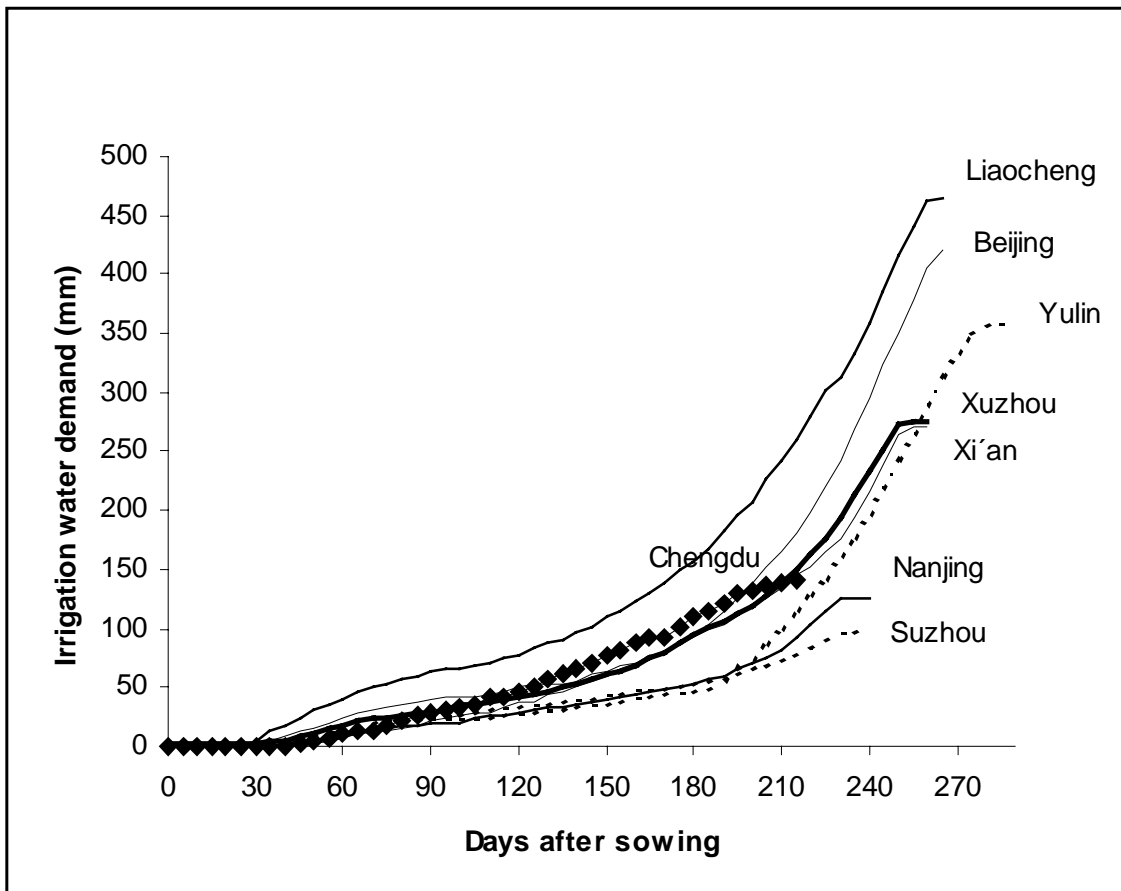


Figure 4. Effect of nitrogen fertilizer and irrigation on wheat yields at Liaocheng and Nanjing. Yield (I=0): Yield with 0 mm supplemental irrigation; Yield (I=420): Yield with 420 mm supplemental irrigation (optimal irrigation level); Yield (N=0): Yield with 0 kg ha⁻¹ of nitrogen fertilizer; Yield (N=180): Yield with 180 kg ha⁻¹ of nitrogen fertilizer (optimal fertilization level).

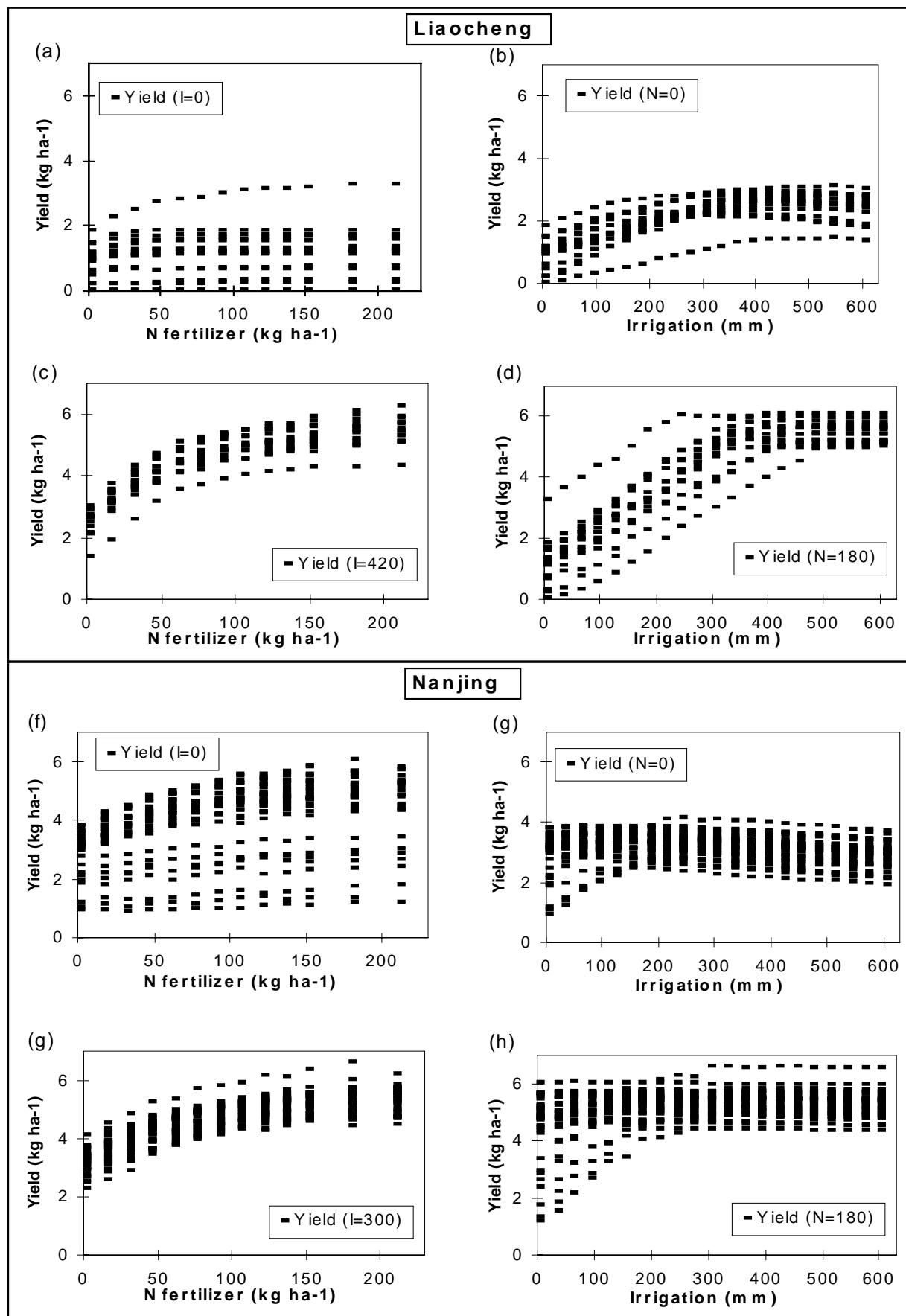


Figure 5. Effect of variation in the observed temperature during the anthesis period (month 5) and growing season precipitation on simulated dryland and fully irrigated wheat yields at Chengdu.

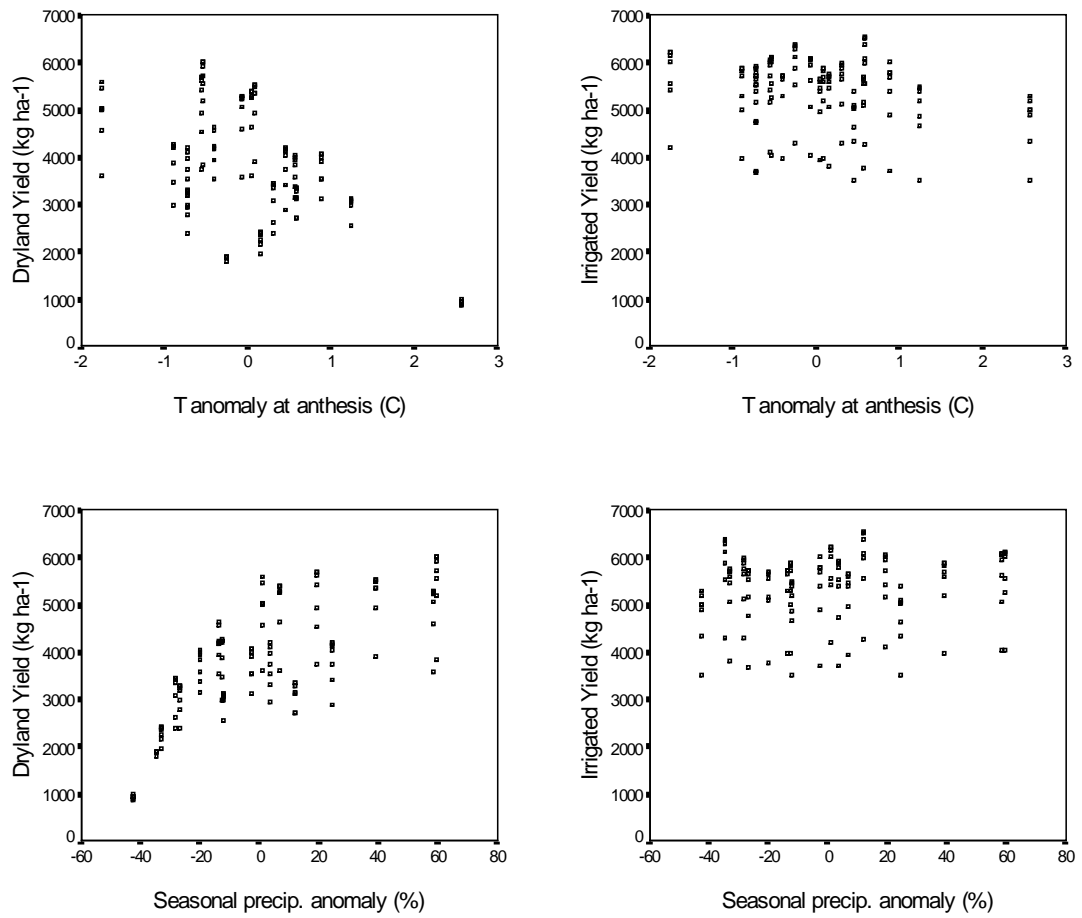
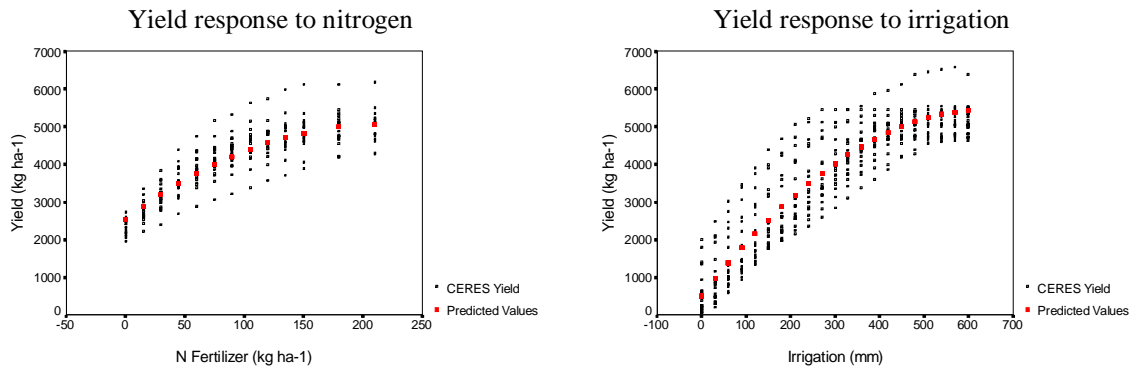


Figure 6. CERES-Wheat and predicted yields with Quadratic non-linear regression models at Beijing.

Quadratic 1: $Y_i = \alpha_1 + \alpha_2(N_i) + \alpha_3(I_i) + \alpha_4(N_i)^2 + \alpha_5(I_i)^2 + \alpha_6(N_i I_i)$



Quadratic 2: $Y_i = \alpha_1 + \alpha_2(N_i) + \alpha_3(I_i + P_i) + \alpha_4(N_i)^2 + \alpha_5(I_i + P_i)^2 + \alpha_6(N_i(I_i + P_i))$

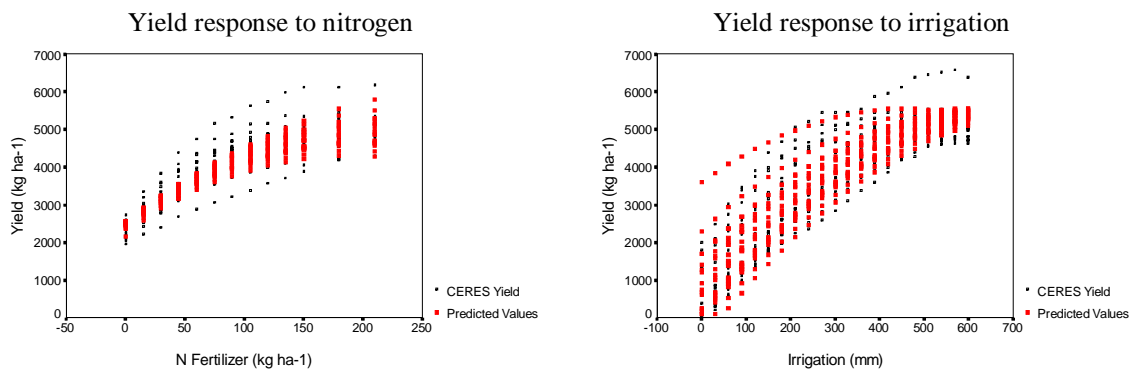
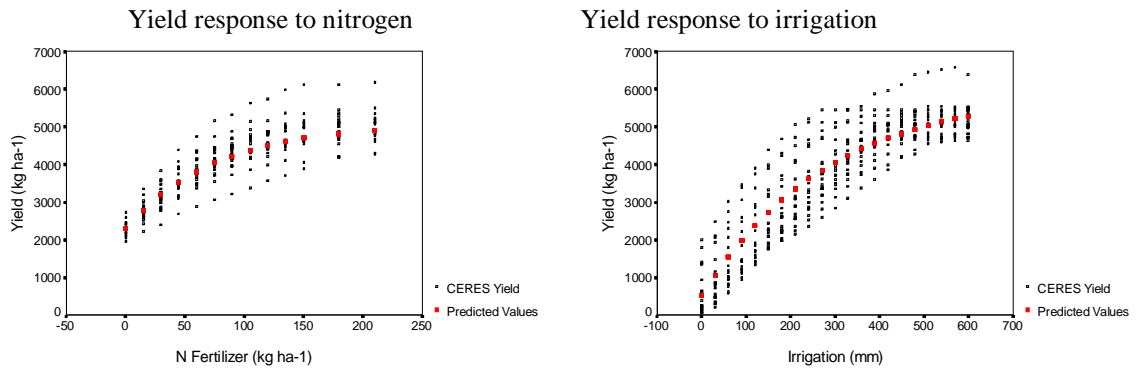


Figure 7. CERES-Wheat and predicted yields with Mitscherlich-Baule models at Beijing.

Mitscherlich-Baule 1:
$$Y_i = \beta_1 * (1 - \exp(-\beta_2 (\beta_3 + Ni))) * (1 - \exp(-\beta_4 (\beta_5 + Ii)))$$



Mitscherlich-Baule 2:
$$Y_i = \beta_1 * (1 - \exp(-\beta_2 (\beta_3 + Ni))) * (1 - \exp(-\beta_4 (\beta_5 + (Ii + Pi))))$$

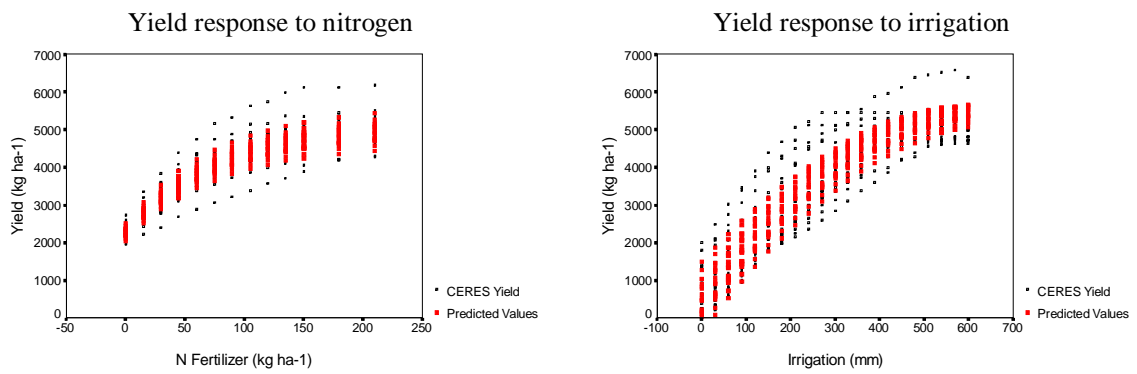
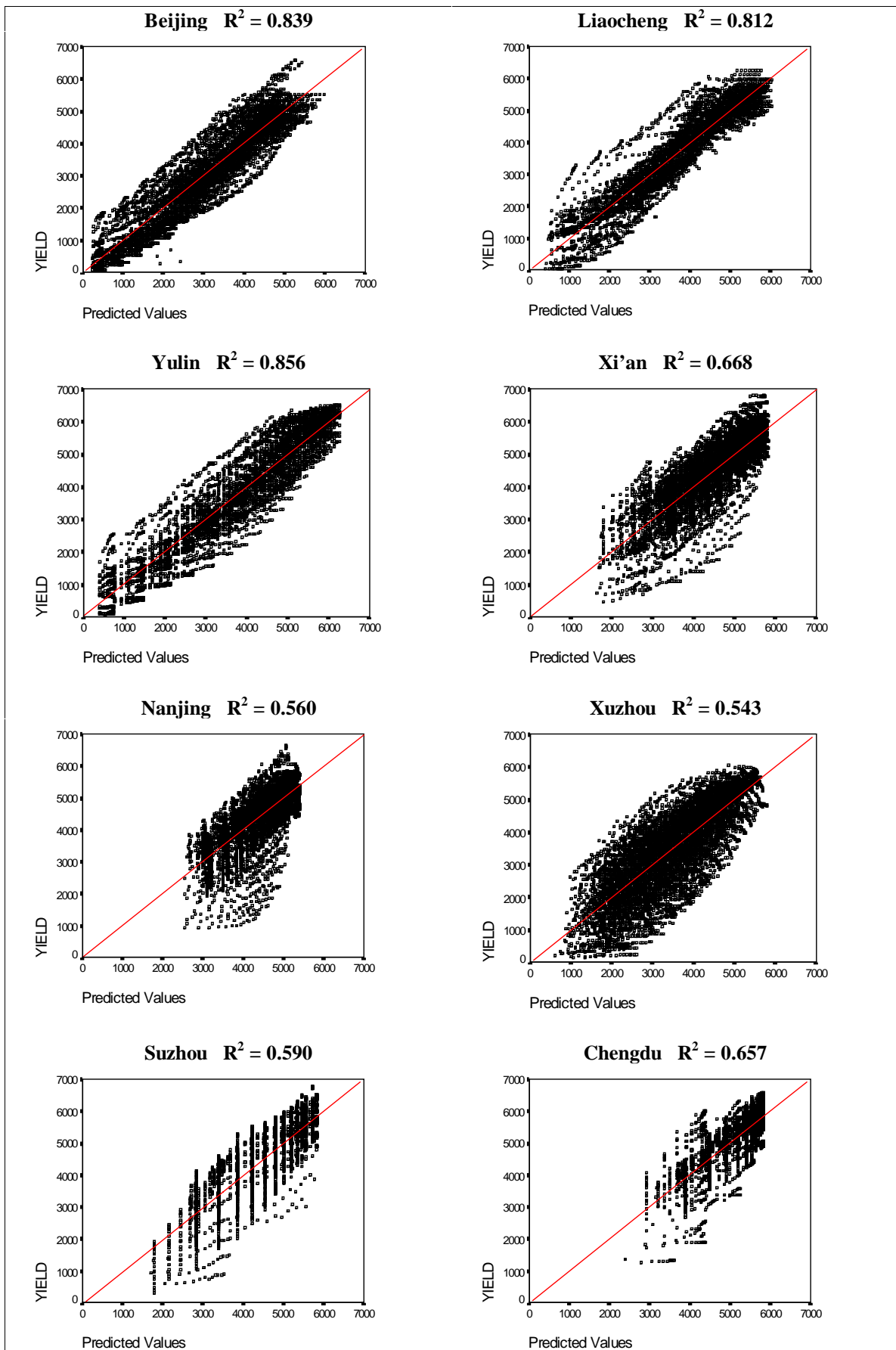


Figure 8. Comparison of yields simulated with the CERES-Wheat model and predicted with the Mitscherlich-Baule 2 model.



Values on kg ha⁻¹.

